



# Controlled flotation processes: Prediction and manipulation of bubble- particle capture

by J. Ralston\*

## Synopsis

The processes by which particles and bubbles interact capture many of the central concepts of colloid science and hydrodynamics. This area of research embraces hydrodynamics, interfacial (including capillary) forces, particle and bubble behaviour and solution chemistry. In this review, we discuss collision, attachment and stability efficiencies. We deal with the identification of a flotation 'domain', the deformation of a bubble surface upon interaction with a solid surface, the kinetics of three phase contact line expansion and the determination of attachment efficiencies through to the direct measurement of bubble-particle interaction forces. We have recently carried out a test of collision theory where the latter embraces both inertial and centrifugal forces. The real challenge is now to quantitatively describe the behaviour of real systems and to incorporate a reliable description of the behaviour of particles in flotation froths. The approach described is very robust when applied to flotation, both from qualitative and quantitative points of view, providing an intellectual foundation for understanding this complex process in separation science and technology.

## Introduction

The capture of particles by rising bubbles is the central process in froth flotation. For efficient capture to occur between a bubble and a hydrophobic particle, they must *firstly* undergo a sufficiently close encounter, a process which is controlled by the hydrodynamics governing their approach in the aqueous environment in which they are normally immersed. Should they approach quite closely, within the range of attractive surface forces, the intervening liquid film between the bubble and particle will drain, leading to a critical thickness at which rupture occurs. This is then followed by movement of the three phase contact line (the boundary between the solid particle surface, receding liquid phase and advancing gas phase) until a stable wetting perimeter is established. This sequence of drainage, rupture and contact line movement constitutes the *second* process of attachment.

A stable particle-bubble union is thus formed. The particle may only be dislodged

from this state if it is supplied with sufficient kinetic energy to equal or exceed the detachment energy, i.e. a *third* process of detachment can occur.

The capture (or collection) efficiency  $E$  of a bubble and a particle may be defined as

$$E = E_C \cdot E_A \cdot E_S \quad [1]$$

where  $E_C$  is the collision efficiency,  $E_A$  is the attachment efficiency and  $E_S$  is the stability efficiency of the bubble-particle aggregate. This dissection of capture efficiency into three process efficiencies was proposed by Derjaguin and Dukhin<sup>1</sup> and focuses attention on the three zones of bubble-particle capture where, in order, hydrodynamic interaction, interfacial forces and bubble-particle aggregate stability are dominant, as illustrated in Figure 1. We should note that these zones are not discrete, rather they grade into one another.

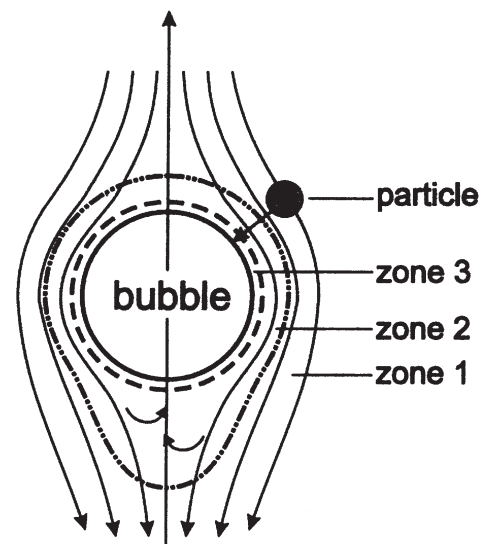


Figure 1—Hydrodynamic (1), diffusiophoretic (2) and surface force (3) zones of interaction between a bubble and a particle (from Ref. 1 with permission)

\* Ian Wark Research Institute, University of South Australia, The Levels, Adelaide, South Australia.  
© The South African Institute of Mining and Metallurgy, 1999. SA ISSN 0038-223X/3.00 + 0.00. Paper received Jul. 1998; revised paper received Aug. 1998.

# Controlled flotation processes: Prediction and manipulation of bubble-particle capture

In this review, we describe each of the substeps in the froth flotation process. The individual processes and efficiencies are focused upon, for they provide the key to understanding the substeps. Our knowledge of the various efficiencies has been enhanced by a continuous, strong research thrust, catalysed by Sutherland<sup>2</sup> in 1948, which resulted in major advances in our understanding in this interdisciplinary field of colloid and flotation science.

## Processes and substeps

### Stability efficiency and detachment

#### Flotation limits for coarse particles

The essential problem in understanding bubble-particle aggregate stability is to determine whether or not the adhesive force, acting on the three phase contact line, is large enough to prevent the destruction of the aggregate under the *dynamic* conditions which exist in flotation.

It is important that the reader understands the physics of the problem before moving on to a mathematical description. Let us consider a smooth spherical particle located at the fluid interface. Once the equilibrium wetting perimeter has been established following spreading of the three phase contact line, the static buoyancy of this volume of the particle will act against the gravitational force (Figure 2). The hydrostatic pressure of the liquid column of height  $Z_0$  acts against the capillary pressure. The 'other detaching forces' require further discussion—since they arise from the particle motion relative to the bubble, velocity dependent drag forces will oppose the detachment of the particle from the bubble. An analysis of these forces is extremely complex and has not been reported to date. Therefore, any force balance will necessarily be quasistatic and approximate.

The net adhesive force,  $F_{ad}$ , is equal to the sum of the attachment forces,  $F_a$ , minus the detachment forces,  $F_d$ , i.e.,

$$F_{ad} = F_a - F_d \quad [2]$$

An equilibrium position is achieved if  $F_{ad}$  is zero. The particle will not remain attached to the bubble if  $F_{ad}$  is negative but will report to the liquid phase.

The mathematical description of the various forces which dictate the equilibrium position of particles at liquid-vapour or liquid-liquid interfaces has followed an evolutionary trail. Analogous processes of interest, for example, include pigment 'flushing', where a solid particle is induced to transfer from one liquid phase to another by appropriate surface modification with surfactants and the stabilization of emulsion droplets by solid particles.

The actual problem of the balance of forces operating on a particle at a liquid-air interface has its historical origins in the work of Wark<sup>3</sup> and Kabanov and Frumkin<sup>4</sup>, who considered the case of a gas bubble attached to a plane solid surface of infinite extent and used this as a model for bubble-particle adhesion in flotation. Since this early work there have been notable contributions from Scheludko<sup>5</sup> and others. It was Princen<sup>6</sup> who proposed the first extensive and generalized treatment of the forces acting on a particle at fluid interfaces. This theory was developed further by Schulze in 1977<sup>7</sup> and expanded in 1984<sup>8</sup>.

It is now pertinent to consider the case of a spherical particle at liquid-air interface. The force balance will be used and then linked to the energy balance. We assume that the system is in a quasistatic state and that the contact angle corresponds to that obtained for a static system. The dynamic contact angle can depart significantly from the static value, depending in part on the velocity of the three phase line of contact. If the particle oscillates around its equilibrium position, the tpic would be expected to move to some extent.

Hence, a full analysis would need to account for the velocity dependent drag forces mentioned above and link these to contact angle dynamics. This is not a tractable problem at present so that a simpler approach is necessary.

Let us suppose that a spherical particle of radius  $R_p$  is attached to a bubble of radius  $R_b$  where  $R_b$  is much greater than  $R_p$ , as shown in Figure 2. From understanding the forces (e.g. capillary, buoyancy, capillary pressure, etc.) which operate on the particle, it is possible to calculate the energy of detachment.

The energy of detachment,  $E_{det}$ , corresponds to the work done in forcing a particle to move from its equilibrium position,  $h_{eq}(\omega)$  at the liquid-vapour interface to some critical point,  $h_{crit}(\omega)$ , where detachment occurs and the particle moves into the liquid phase. The sum of the various forces,  $\Sigma F$ , is related to  $E_{det}$  by:

$$E_{det} = \int_{h_{eq}(\omega)}^{h_{crit}(\omega)} \Sigma F dh(\omega) \quad [3]$$

The detachment process takes place when the kinetic energy of the particle equals  $E_{det}$ . The kinetic energy of the particle is given by  $2/3\pi R_p^3 \rho_p V_t^2$ , where  $V_t$  is the relative (turbulent) velocity of the particle, acquired due to stresses on the bubble-particle aggregate in the turbulent field of the flotation cell, as the aggregate collides with other bubbles or aggregates or due to other modes of excitation.  $V_t$  corresponds to the velocity of gas bubbles in the flotation cell.  $\rho_p$  and  $\rho_f$  refer to the densities of the particle and fluid respectively.

The maximum floatable particle diameter based on the kinetic theory,  $D_{max,K}$ , is given as:

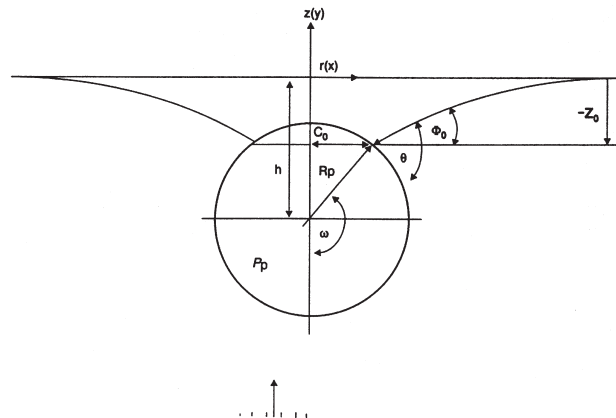


Figure 2—Location of a smooth spherical particle at a fluid interface (from Ref. 8 with permission)

# Controlled flotation processes: Prediction and manipulation of bubble-particle capture

$$D_{\max, K} = 2 \left[ \frac{3}{2\pi\rho_p V_r^2} \int_{h_{eq}(\omega)}^{h_{crit}(\omega)} \left\{ \frac{2}{3} \pi_p^3 \rho_p g \right\} \right. \\ \times \left( 1 - \frac{2\rho_p}{\rho_f} - \cos^3 \omega + \frac{3h}{2R_p} \sin^2 \omega - \frac{3}{a^2 R_p^2} \sin \omega \sin(\omega + \theta) \right) \\ \left. - \pi (R_p \sin \omega)^2 \left( \frac{2\gamma}{R_b} - 2R_b \rho_p g \right) \right]^{1/3} \quad [4]$$

Equation [4] may also be solved by numerical integration or by plotting each of the kinetic and detachment energies as a function of  $R_p$  at constant  $\gamma$  and  $\rho_p$  and specified  $V_r$ .

This equation has been shown to adequately describe the detachment of a sphere from a liquid-vapour interface by Schulze<sup>6</sup> as well as the behaviour of hydrophobic angular quartz particles, between approximately 35 to 120  $\mu\text{m}$  in diameter, under flotation conditions by Crawford and Ralston<sup>9</sup>.

## Flotation limits for fine particles

The only theoretical study to date dealing with the limit of floatability of fine particles was proposed by Scheludko and his colleagues<sup>5</sup>. The limit is the critical work of expansion required to initiate a primary hole or three phase contact line during bubble-particle approach, a requirement which is met by the kinetic energy of the particles. The matching of these two quantities enables a minimum particle diameter,  $D_{\min, K}$  for flotation to be obtained.

$$D_{\min, K} = 2 \left[ \frac{3\kappa^2}{V_r^2 \Delta\rho\gamma \{1 - \cos\theta\}} \right]^{1/3} \quad [5]$$

where  $K$  is the line tension, opposing expansion of the three phase contact. It was Gibbs who first identified the importance of line tension, using as an example the line of intersection of the three surfaces of discontinuity which exist when two gas bubbles adhere together.

Molecules which are present in a line have a free energy which is different from those at a surface; in fact there is an excess linear free energy and a linear tension in an analogous fashion to that of excess free energy and surface tension.

In fact,

$$\kappa = \left( \frac{\partial F}{\partial L} \right)_{T, V, W} \quad [6]$$

where  $F$  is the Helmholtz free energy,  $L$  is the contact line, and  $W$  is the thermodynamic work. The Young-Dupre equation becomes:

$$\gamma_{S/V} - \gamma_{S/L} = \gamma_{L/V} \cos\theta \pm \frac{\kappa}{r} \quad [7]$$

The line tension is important for small contact radii and can oppose or reinforce  $\gamma_{L/V} \cos\theta$ . It counteracts the formation of the three phase contact line in Scheludko's theory, the latter neglecting thin film drainage and other hydrodynamic effects. The experimental data of Crawford and Ralston<sup>9</sup> for hydrophobic, angular quartz particles between about 10 to 30  $\mu\text{m}$  in diameter follow a general trend which is predicted by Equation [5]. Drelich and Miller<sup>10</sup> have shown that acceptable agreement is achieved if a pseudo-line tension, embracing surface heterogeneities, replace  $\kappa$  in Equation [5].

This in turn enables  $D_{\min}$  in Equation [5] to be re-expressed in terms of a critical bubble radius below which attachment does not occur. Reconciliation between theory and experiment is then achieved, although the concept of pseudo-line tension needs to be placed on a firmer experimental footing.

## Attachment efficiency

Derjaguin and Dukhin<sup>1</sup> identified zone 2 in Figure 1 as that region where diffusion effects are important. A strong electric field exists in this zone, for the liquid flow around the moving bubble gives rise to a tangential stream at its surface which destroys the equilibrium distribution of adsorbed ions there. Where surfactant is present it is continually swept from the upper to the lower surface of the bubble. Transport of ionic surfactant to the moving bubble surface therefore takes place, leading to the establishment of a concentration gradient.

A strong electric field of order  $3000 \text{ V cm}^{-1}$  is established when the cation and anion diffusion coefficients differ, as they generally do. Hence charged particles entering zone 2 will experience an electrophoretic force in precisely the same way as in an electrophoresis cell and would be either attracted towards, or repelled from the bubble surface. Derjaguin and Dukhin coined the term 'diffusiophoresis' for this phenomenon i.e. the 'diffusiophoretic force' therefore acts on the particle as an additional force.

To date however, evidence confirming the presence or absence of diffusiophoresis in flotation is equivocal and sparse. Apart from noting its possible contribution to capture efficiency it is not pursued further here.

In zone 3, surface forces predominate once the thin film between the bubble and the particle is reduced much below a few hundred nanometre. These forces can *accelerate*, *retard* or even *prevent* the thinning of the liquid film between the particle and the bubble. From a thermodynamic point of view, the free energy of a liquid film differs from the bulk phase from which it is formed. This excess free energy was originally called the 'wedging apart' or 'disjoining' pressure by Derjaguin and represents the difference between the pressure within the film,  $p^f$  and that in the bulk liquid adjacent to the solid surface,  $p^1$ . Note that for a bubble pushed against a flat solid surface, immersed in water,  $p^b$ , the pressure within the bubble, is equal to  $p^f$ . Derjaguin and Titievskaya<sup>11</sup> and Scheludko *et al.*<sup>12</sup> performed experimental measurements of disjoining pressures, providing both the first real verification of the DLVO theory of surface forces, as well as the first accurate experimental estimates of the Hamaker constant, respectively. The disjoining pressure ( $\pi$ ) depends on the film thickness,  $h$ , and:

$$\pi(h) = p^f - p^1 \quad [8]$$

For mechanical equilibrium in a stable film  $\pi(h) > 0$  and  $d\pi/dh < 0$ .

If the liquid film is stable at all thicknesses the liquid is said to completely wet the solid. This occurs, for example, when an air bubble approaches a clean silica surface immersed in water—in this instance the Hamaker constant is negative and the corresponding Van der Waals force is repulsive for the silica/water/air triple layer.

## Controlled flotation processes: Prediction and manipulation of bubble-particle capture

For an unstable film the thin film must drain then rupture and the resulting three phase line of contact (tpic, vapour-water-solid) must expand to form a wetting perimeter before the particle can adhere to the bubble.

Each of these events will have a characteristic time associated with them, the sum of which must be less than the contact time between the bubble and the particle if flotation is to occur. The contact time is generally of the order of  $10^{-2}$  seconds or less.

The induction time,  $\lambda$  is normally taken as the time required for bubble-particle adhesion to occur, once the two are brought into contact, i.e. it is the sum of the thin film drainage and tpic spreading times ( $t_{\text{film}} + t_{\text{tpic}}$ ) and is synonymous with the attachment time. Rupture is a very fast process and is not a significant contributor to  $\lambda$ .

When a bubble is pressed against a solid surface, through water, the intervening film is generally not plane parallel. Rather the edge of the film thins quickly and a small, thicker dimple is trapped in the centre, for the bubble is deformable. This is essentially a kinetic phenomenon, caused by the flow being greatest at the very edge of the film in the initial stages of drainage. The existence of this dimple has been detected by techniques such as laser interferometry<sup>13</sup>. Hydrodynamic theories attempting to describe the profile and evolution of the dimple have been proposed but with very limited success in describing experimental data. Surface deformation of bubble surfaces can also occur under the influence of electrostatic interactions, (and possibly other surface forces as well) aside from any kinetic effects, as shown by Miklavcic, Horn and Bachmann<sup>14</sup>.

An unstable film arises when there is a net attractive force between the particle and the bubble. This normally occurs when there is an attractive hydrophobic force involved, for the Van der Waals and electrostatic forces (the 'DLVO' components) are repulsive, except in rare circumstances. The measurement of this hydrophobic force and its theoretical origins are subjects of intense research effort. In recent times it has become possible to measure the hydrophobic force, in a configuration relevant to the flotation process, by attaching a small particle to the cantilever in an atomic force microscope (Figure 3). The particle is then pressed against a captive bubble and the force-separation distance profile determined, for example, as shown by Fielden, Hayes and Ralston<sup>15</sup>. In this fashion, the various surface forces may be explored.

Experimental evidence relating to film drainage in systems where soluble surfactants are present is rather equivocal. Adsorption and desorption processes coupled with possible molecular reorientation make any theoretical interpretation difficult. Unfortunately, these are the very systems which are of primary interest to mineral processing. Furthermore, additional complications ensue when one considers a particle approaching a bubble in flotation.

The nature of the bubble surface (i.e. whether it is mobile or immobile) will influence the evolution of the thin film between bubble and particle. This makes any solution of the equation for film drainage difficult, particularly in the case of the angular particles that are normally present in flotation. It is worth recalling at this point, the observations that smooth spheres float more slowly than angular particles under otherwise identical conditions, presumably because the

asperities on the angular particles lead to increased film drainage rates and/or rupture<sup>16,17</sup>.

The kinetics of movement of the three phase line of contact (tpic) are of central importance in many processes, apart from flotation. During the movement of the tpic a dynamic contact angle is established. Irrespective of whether the 'surface chemical', 'hydrodynamic' or mixed 'surface chemical/hydrodynamic' approaches are used there is as yet no general theory which adequately describes tpic kinetics on all surfaces<sup>18,19</sup>. One cannot generally calculate *ab initio* what the spreading velocity of the tpic will be when an air bubble spreads over a mineral surface immersed in water in the presence of a surfactant. Part of the problem, at least, is due to the fact that poorly characterized experimental systems have been used, where any generalization has been obscured by the same time-dependent adsorption/desorption/molecular reorientation processes which complicate thin film drainage rate studies. Physical and chemical surface heterogeneities on the particle surface also strongly influence the tpic kinetics.

At present only the crudest estimates of  $t_{\text{film}}$  and  $t_{\text{tpic}}$  can be made. Hence various experimental methods for determining  $\lambda$  are frequently resorted to. Ye and Miller<sup>20</sup> have developed a potentially valuable approach to the determination of contact times, based on bubble deformation and restoration.

These experimental methods for determining induction times are generally based on either pressing a bubble against a smooth mineral surface or against a bed of particles. The disadvantages of all current methods for determining  $\lambda$  include: (1) insufficient understanding of the process of bubble deformation and energy dissipation during bubble/particle collision; (2) insufficient information concerning the behaviour of the attractive hydrophobic forces during the bubble/particle interaction (e.g. how the thin film of liquid evolves with time, during the time a particle slides or rolls around a bubble; it may well be incorrect to assume that bubble-particle interaction ceases when the particle passes the bubble equator<sup>8,20</sup>); (3) data on  $t_{\text{film}}$  e.g. influence of surfactant type and concentration on thin-film drainage mechanisms and rate; and (4) data on  $t_{\text{tpic}}$  as a function of hydrophobicity, physical and chemical surface heterogeneities and surfactant type.

The most appropriate method for determining induction times is probably through direct observation of bubble/particle interactions in a flotation cell under well-

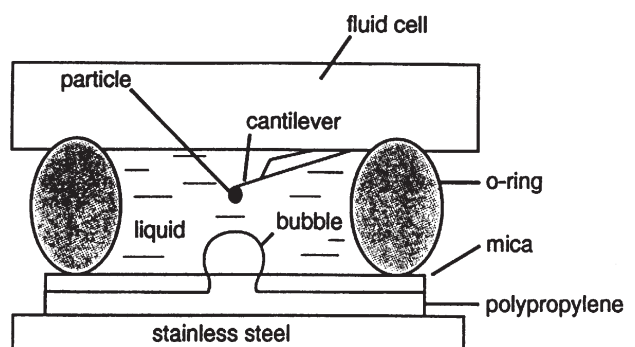


Figure 3—Experimental arrangement for the measurement of forces between a particle and a bubble using the atomic force microscope colloid probe technique (from Ref. 15 with permission)

# Controlled flotation processes: Prediction and manipulation of bubble-particle capture

defined conditions. The necessary theory can then be developed. For the present the Sutherland<sup>2</sup> and similar approaches serve as useful approximations in determining  $\lambda$  from experimental flotation data of the type normally generated.

Kinetic effects certainly have a strong influence on bubble-particle collision and attachment efficiencies. The latter provides the key to selective separations in flotation.

## Collision efficiency

For a batchwise flotation process, the flotation recovery (the mass of particles recovered in a given time)  $R$  is given by

$$R = 1 - \exp\left(\frac{-t3GE_cE_AE_S h}{2d_bV}\right) \quad [9]$$

where  $G$  is the volumetric gas flow rate of a swarm of bubbles of diameter  $d_b$  passing through a particle suspension of volume  $V$  and depth  $h$  and

$$k = \frac{3GE_cE_AE_S h}{2d_bV} \quad [10]$$

The flotation rate constant  $k$  is directly analogous to that obtained in chemical reaction kinetics. Its value will be partly determined by the substeps(s) in bubble-particle collision, attachment and detachment processes, as well as by physical variables such as  $G^*$ .

Equation [9] has been shown by Collins and Jameson<sup>21</sup> to apply to a system of monodisperse polystyrene latex particles, for example, floating under batchwise conditions. A plot of  $\ln(1-R)$  versus  $t$  yields the rate constant  $k$ . For systems which are polydisperse in particle size and/or in which particles of different hydrophobicities are present, the recovery then becomes the sum of a series of exponential terms and the plot of  $\ln(1-R)$  versus  $t$  will show curvature, reflecting the different contributions from the various particles in the pulp to the recovery.

## Bubble surface mobility

In the hydrodynamics of particle-bubble collision, most efforts have focused on the regime where the bubble surface is immobile (or strongly retarded) caused either by intentional surfactant addition or by the adsorption of impurities from the water. The effect of the long range hydrodynamic interaction (LRHI) under conditions where inertia is very small, was convincingly demonstrated by Collins and Jameson<sup>21</sup> and Reay and Ratcliff<sup>22</sup> in their flotation experiments. The most important manifestations of the LRHI revealed experimentally are rapid decreases in  $E_c$  as the particle size decreases and the bubble size increases. Satisfactory agreement between the theory of particle-bubble collision and experiment was established by Anfruns and Kitchener<sup>23</sup>. However, this relates to the regime with a strongly retarded bubble surface because the bubble radius in their experiments was rather small ( $0.4 \times 10^{-3}$  to  $1 \times 10^{-3}$  m) and the water used containing traces of surface active impurities, as acknowledged by the authors. Mathematical modelling of the hydrodynamic field created by a rising

bubble at intermediate values of Reynolds number ( $Re$ ) has been performed by different groups<sup>24,25,33</sup>. This has permitted (e.g.<sup>6-8</sup>) both an equation for collision efficiency for intermediate  $Re$  values as well as models for particle sliding (e.g.<sup>29,30</sup>) to be derived.

In mentioning these investigations, the assumption that total retardation of the bubble surface (i.e. immobility) under industrial conditions is generally made. In contrast, Schulze<sup>31</sup> suggests that the problem of the degree of the bubble surface retardation is *not* solved and a large uncertainty exists when collision theory is applied in a flotation operation in industry. At sufficiently low surfactant concentrations, the surface of bubbles which are not too small is mobile. Systematic experimental investigations of particle-bubble collision under conditions of rising, mobile bubble surfaces started only recently<sup>32</sup> in contrast to studies of retarded bubble surfaces. Any section of the mobile bubble surface is in a state of permanent expansion. It can cause a qualitative change in the mechanism of thin layer drainage and affect its stability. For example it may increase the value of the critical thickness,  $h_{cr}$ . In addition to this feature, which is of fundamental significance for thin film dynamics, the collision efficiency is enhanced. Bubble surface retardation decreases collision efficiency approximately ten times<sup>31</sup> thus the situation where attention has been paid almost exclusively to the retarded collision rate is surprising. In this review, we will mainly emphasise the collision process enhanced due to bubble surface mobility.

## Significance of inertial forces in collision

Inertial forces are usually neglected because the traditionally used assumption of surface retardation corresponds to moderately small to intermediate size bubbles in the presence of surfactants and because both liquid and particle movement is retarded near the bubble surface. The possibility of high velocities for medium size particles and bubbles where inertial forces<sup>27,29</sup> may not be neglected is generally overlooked. A rare exception is the work of Dobby and Finch<sup>33</sup> where attention is paid to the inertial deposition of particles on a retarded bubble surface and the Stokes number is taken into account. The dimensionless Stokes number  $K$  characterizes the ratio of the magnitude of the inertial force to the viscous resistance of the medium, which appears as the particle is deposited onto the bubble surface from the flow

$$K = \frac{2}{9} \rho U_b a_p^2 / a_b \eta \quad [11]$$

where  $\eta$  is the dynamic viscosity;  $\rho$  is the density of the particle;  $U_b$  is the velocity of the rising bubble and  $a_p$  and  $a_b$  are particle and bubble radii, respectively.

If one considers the depositing particle to be a material (or, better, mass) point, Levin<sup>34</sup> showed that the inertial deposition of particles with sizes less than a certain critical dimension, corresponding to the critical Stokes number value  $K_c$  where

$$K_c = \frac{1}{12} \quad [12]$$

is impossible. This analytical result agrees with Langmuir's numerical calculations<sup>35</sup>. The essential role of inertial particle

\*For a constant  $G$  and constant bubble size distribution,  $d_b$  will be an appropriate average

# Controlled flotation processes: Prediction and manipulation of bubble-particle capture

deposition has been verified and described quantitatively for Stokes numbers above the critical value<sup>33</sup>. At subcritical Stokes numbers, various authors have essentially used inertialess flotation theories (e.g.<sup>26, 47</sup>) to describe bubble-particle interaction. It can be demonstrated that inertial forces *can* manifest themselves even at subcritical Stokes numbers under conditions where the bubble surface is free<sup>36</sup>. Furthermore, for large bubbles with high velocities, the tangential fluid velocity at the surface is as high as the bubble rising velocity. Thus the problem that we must consider is a rather new and complicated problem of the inertial-hydrodynamic interaction. This problem is not new if one neglects the particle dimension and replaces it by a mass point. Langmuir<sup>35</sup> first considered the inertial-hydrodynamic interaction of a small droplet with a large falling droplet within its hydrodynamic field. To overcome the mathematical difficulties involved, he replaced the particle by a mass point. In Derjaguin and Dukhin<sup>37</sup>, the analogy between the Langmuir model and particle-bubble collision was pointed out for the situation where the hydrodynamic fields around either a rising bubble or a falling larger drop are identical. Langmuir approximated the results of his numerical calculations by a formula for the collision efficiency:

$$E = \frac{K^2}{(K + 0.2)^2} \quad [13]$$

This was confirmed in papers in which the finite size of the particles was taken into account<sup>38,39</sup>. With decreasing particle size and a corresponding decrease in inertial forces and the Stokes number  $K$ , the inertial deposition of particles from the flow onto the bubble surface becomes weaker.  $E$ , according to Equation [13], drops off rapidly with decreasing  $K$ . This relationship has now been confirmed experimentally, not only qualitatively but also quantitatively (for  $K < 0.7$ )<sup>40</sup>.

The departure from the mass point idealization leads to quite another picture of the collision process. When the finite size of the particles is taken into account, deposition is possible, according to Sutherland<sup>2</sup> with any particle size, and deposition is characterized by the formula.

$$E_o = 3a_p / a_b \quad [14]$$

From this we can conclude that the theory constructed using the mass point approach, while it is useful with values of  $K$  that are reasonably large, becomes unsuitable for small  $K$ . Conclusions concerning the absence of inertial forces in considerations of collision efficiency<sup>41</sup> at small  $K$  may not be valid, for they arise from the particle being described as a mass point. Note that the calculations of  $E$  by Fonda and Herne<sup>38</sup> and Michael and Norey<sup>39</sup> were performed with  $K > 0.1$ , i.e. with  $K > K_c$ . Experimental tests of Langmuir's formula also covered only values where  $K > K_c$ <sup>40</sup>. Agreement between the theory of particle-bubble collision and experiment exists for the case of inertialess flotation<sup>22,41</sup> where

$$K \ll K_c \quad [15]$$

and for the inertial deposition of large particles onto the rising bubble<sup>40</sup> where

$$K \gg K_c \quad [16]$$

In inertialess flotation, collision occurs due to interception<sup>2</sup> and the collision efficiency is a function of the ratio of particle size to bubble size, i.e.

$$E = E(a_p / a_b) \quad [17]$$

as was first established by Sutherland<sup>2</sup>. Under inertial deposition the collision efficiency depends on the Stokes number,  $K$ , as is seen from Equation [13] and the mass point approach can be used (at large  $K$ )

$$E = E(K) \quad [18]$$

For intermediate particle dimensions under conditions where

$$K \approx K_c \quad [19]$$

the role of inertial forces cannot, a priori, be excluded. In other words the collision efficiency is expected to be a function of two arguments

$$E = E(a_p / a_b, K) \quad [20]$$

This expectation is confirmed by both experiment and theory<sup>36</sup>. Under conditions where  $K \ll K_c$  the equation derived approaches the Sutherland equation. Thus, the Sutherland theory may be generalized by the incorporation of weak inertial forces. Note that weak inertial forces produce a large change in collision efficiency when  $K \approx K_c$ . A new mechanism for the inertial hydrodynamic bubble-particle interaction has been established<sup>36</sup>. The qualitatively new and unexpected peculiarity of the particle-bubble interaction at the critical Stokes number is the *negative* influence of the inertial forces on the particle-bubble interaction. In contrast to inertial deposition at high Stokes numbers, where the collision efficiency increases with  $K$  in the regime under investigation, it turns out that the inertial forces influencing the collision efficiency cause a decrease in the latter in comparison with the Sutherland equation.

In this review, we restrict our considerations by either Equation [15] or condition [19], thus small surface deformations are neglected. Strong deformation of the bubble surface at supercritical Stokes numbers must still be addressed<sup>24,43</sup>.

We have shown<sup>36</sup> that the essential problem in the hydrodynamics of the elementary flotation act for small particles is the calculation of their trajectory close to the surface. Thus

$$\frac{E_c}{E_o} = \sin^2 \theta_t \exp \left[ 3K^{III} \cos \theta_t \left( \ln \frac{3}{E_o} \pm 1.8 \right) - \frac{9K^{III} \left( \frac{2}{3} + \frac{\cos^3 \theta_t}{3} - \cos \theta_t \right)}{2E_o \sin^2 \theta_t} \right] \quad [21]$$

where  $\theta_t$  and  $K^{III}$  are given by

$$\theta_t = \arcsin \left\{ 2\beta \left( \sqrt{1 + \beta^2} - \beta \right) \right\}^{\frac{1}{2}} \quad [22]$$

where  $\theta_t$  is the angle of tangency and

$$K^{III} = \frac{\Delta\rho}{\rho} . K = \frac{2U_b . \Delta\rho . a_p^2}{9\eta a_b} \quad [23]$$

# Controlled flotation processes: Prediction and manipulation of bubble-particle capture

with the dimensionless number  $\beta$  defined as

$$\beta = \frac{2 \cdot E_o \cdot f}{9K^{III}} \quad [24]$$

and  $E_o$  is given in Equation [14];  $\Delta\rho$  is the density difference between the particle and the fluid;  $f$  is a numerical factor which characterizes the short range hydrodynamic interaction between the particle and the free bubble surface. For a free, non-retarded bubble surface,  $f$  equals 2.034<sup>36</sup>.

For convenience and to simplify the comparison between theory and experiment, Equation [21] may be re-expressed as

$$E_c = \left( \frac{E_c}{E_o} \right) \cdot E_o \quad [25]$$

where  $E_c/E_o$  is given by Equation [21] and  $E_o$  by Equation [14].

At high particle hydrophobicity and at rather high electrolyte concentration, the product  $E_a E_s$  approaches its maximum value (i.e. 1) for rather small particles<sup>23,32,44</sup>. At these maximum attachment and stability efficiencies, improvements to flotation can only be achieved due to the enhancement of collision efficiency, a particularly important issue for fine particles. This possible improvement is very promising because the collision efficiency is always very low for relatively large bubbles, such as those encountered in flotation practice. Under conditions where  $E_a E_s \approx 1$ , experimental determination of the collision efficiency is possible by means of its identification with the experimental capture efficiency,  $E^{exp}$ , thus

$$E^{exp} \approx E_c \quad [26]$$

Only under such favourable conditions, where two of the main steps are *controlled*, is a critical, experimental examination of the different hydrodynamic models of particle-bubble collision possible.

## Dependence of collision on particle size

Experimental  $E(d_p)$  curves obtained under conditions<sup>36</sup> of maximum attachment and stability efficiency ( $E_a E_s \approx 1$ ) only are shown, corresponding to high contact angle ( $73^\circ$ ) and high salt concentration ( $10^{-2}M$ ). The data are shown in Figure 4 for a bubble diameter of  $1.52 \times 10^{-3} m$  and in Figure 5 for a diameter of  $0.77 \times 10^{-3} m$ . Theoretical curves based on Equations [14] and [21] are also shown for comparison<sup>36</sup>. There is clearly very good agreement between theory Equation [21] and experiment with a marked divergence from the Sutherland predictions.

## Dependence of collision on bubble size and bubble velocity

In the calculation of theoretical collision efficiency (Figures 4 and 5), bubble velocities of  $31.6 \times 10^{-2} ms^{-1}$  for  $d_b = 1.52 \times 10^{-3} m$  and  $19.6 \times 10^{-2} ms^{-1}$  for  $d_b = 0.77 \times 10^{-3} m$  were used. These values are in agreement with other recent investigations<sup>45,46</sup>.

The difference in bubble velocity does not cause a

significant change in the collision efficiency, a not altogether surprising result because the actual difference in the velocities is only about 20%. However, the difference in bubble velocities at bubble diameters of  $1.52 \times 10^{-3} m$  and  $0.75 \times 10^{-3} m$  is large. Nevertheless, Equation [21] describes the experimental data dealing with two bubble sizes over a range of particle sizes very well (Figures 4 and 5). This is a rather severe test of the theory and the outcome is comfortingly positive. We stress that the very good agreement between theory and experiment applies only at contact angles equal to, or greater than,  $70^\circ$  and at high electrolyte concentrations.

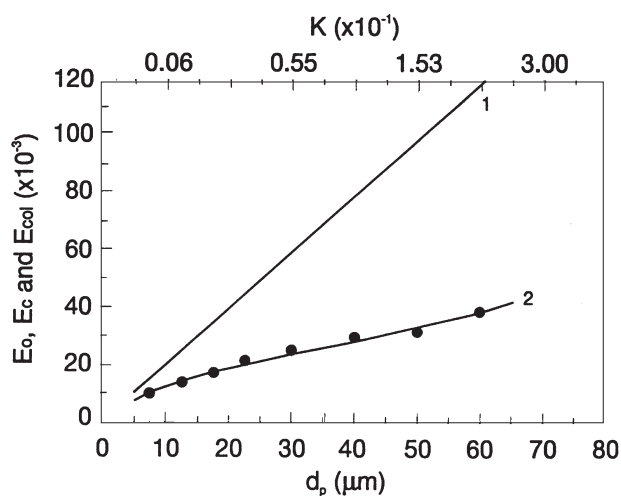


Figure 4—Comparison of collision efficiency calculated according to Sutherland equation ( $E_o$ , equation 14, curve 1) and the Generalized Sutherland Equation ( $E_c, E_q$ , [21], Curve 2).  $K$  is also shown. The experimental data ( $E$ ) with filled circles overlap with the predictions of the GSE. Conditions:  $2a_b = 1.52 \times 10^{-3} m$ ;  $U_b = 31.6 \times 10^{-2} ms^{-1}$ ; pH 5.6;  $[KC1] = 10^{-2} M$ ;  $\theta_a = 73^\circ$ . Bubble Reynolds number is 480. [From Ref. 36, with permission]

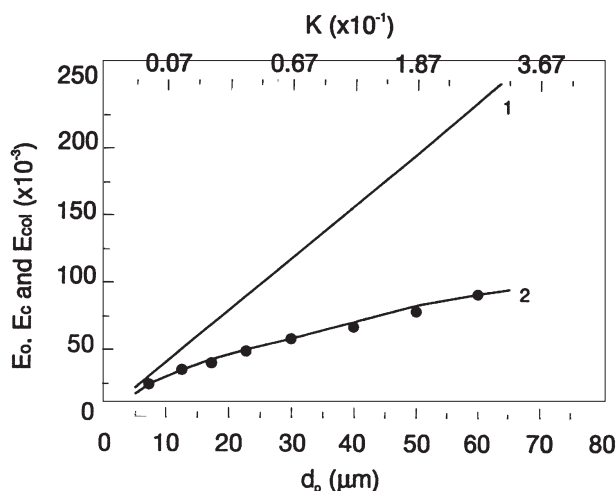


Figure 5—Comparison of collision efficiency calculated according to Sutherland equation ( $E_o$ , Eq. [14], Curve 1) and the Generalized Sutherland Equation ( $E_c$ , Eq. [21], Curve 2). The experimental data ( $E$ ) with filled circles overlaps with the predictions of the GSE. Conditions:  $2a_b = 0.77 \times 10^{-3} m$ ;  $U_b = 19.6 \times 10^{-2} ms^{-1}$ ; pH 5.6;  $[KC1] = 10^{-2} M$ ;  $\theta_a = 73^\circ$ . Bubble Reynolds number is 151. [From Ref. 36 with permission]

# Controlled flotation processes: Prediction and manipulation of bubble-particle capture

## The future

In terms of our fundamental understanding, there is no entirely adequate collision model which correctly accounts for particle size and inertial effects in the presence *and* absence of soluble surfactants. Thin film drainage is poorly understood when one of the interfaces is both physically and chemically heterogeneous, the other deformable. The nature of the hydrophobic interaction between a particle and a bubble requires both experimental and theoretical verification, particularly the influence of dissolved gases. There is no reliable model at present to describe the movement of a three phase contact line over a rough surface. Thus, major research challenges exist which, if they are to be successfully overcome, must embrace systems where surfactants are both present and absent.

From a separation technology point of view, froth flotation will continue to be one of the principal means by which ores are successfully beneficiated for many years to come. Increasingly the technique is also being used in the deinking of paper, soil remediation, plastics recycling and heavy metal ion decontamination, to name but a few examples. Both research and practice are expected to accelerate strongly over future decades as new techniques and theoretical approaches are used.

## References

1. DERJAGUIN, B.V. and DUKHIN, S.S. *Transactions of the Institute of Mining and Metallurgy* 70, (1960-1), p. 221.
2. SUTHERLAND, K.L. *Journal of Physical Chemistry* 52, (1948) p. 394.
3. WARK, I.W. *J. Phys. Chem.*, 37 (1933) p. 623.
4. KABANOV, B. and FRUMKIN, A. *Z. Phys. Chim.*, A165 (1933) p. 433.
5. SCHELUDKO, A., TOSEV, B. and BOGADIEV, B., *J. Chem. Soc. Trans. Faraday* 1, 72 (1976) p. 2815.
6. PRINCEN, A. In: *Surface and Colloid Science*, vol. 2, E. Matijevic (Ed.) *John Wiley*, New York, NY, 1969, Chapter 2.
7. SCHULZE, H.J. *Int. J. Miner. Process.*, 4 (1977) p. 241.
8. SCHULZE, H.J. *Physicochemical Elementary Processes in Flotation*, Elsevier, Amsterdam (1984).
9. CRAWFORD, R. and RALSTON, J. *International Journal of Minerals Processing*, 23, (1988) p. 55.
10. DRELICH, J. and MILLER, J.D. *Colloids and Surfaces* 69, (1992) p. 35.
11. DERJAGUIN, B.V. and TITIEVSKAYA, *Proc. 2nd Int. Cong. On Surface Activity*, 1 (1957) p. 536.
12. SCHELUDKO, A., and EXEROWA, D. *Kolloid, Z.* 168 (1960) p. 24.
13. HEWITT, D., FORNASIERO, D., RALSTON, J. and FISHER, L.R. *J. Chem. Soc. Far. Trans.* 89 (1993) p. 817.
14. MIKLAJVIC, S.J., HORN, R.G. and BACHMANN. *Journal of Physical Chemistry*, 99, (1995) p. 16537.
15. FIELDEN, M.L., HAYES, R.A. and RALSTON, J. *Langmuir*, 12, (1996) p. 3721.
16. ANFRUNS, J.F. and KITCHENER, J.A. *Trans IMM Sect. C*, 86 (1986) C9.
17. BLAKE, P. and RALSTON, J. *Colloid Surf.*, 15 (1985) p. 101.
18. BLAKE, T.D. Chapter 5 in *Wettability*, Edited by J.C. Berg, *Marcel Dekker Inc.*, New York, 1993.
19. HAYES, R.A., and RALSTON, J. *J. Coll. Int. Sci.*, 159, (1993) p. 429.
20. YE, Y. and MILLER, J.D. *International Journal of Mineral Processing*, 25, (1989) p. 199.
21. COLLINS, G.L. and JAMESON, G.J. *Chemical Engineering Science*, 31, (1976) p. 985.
22. REAY, D., and RATCLIFF, G.A. *Can., J. Chem. Eng.*, 53, (1975) p. 481.
23. ANFRUNS, J.P. and KITCHENER, J.L. *Trans. Inst. Mining Metall.*, 86, (1977) C9.
24. MASLIYAH, J.H. Ph.D. dissertation, University of British Columbia, Vancouver, Canada (1970).
25. WOO, S.W. Ph.D. dissertation, McMaster University, Hamilton, Canada (1971).
26. WEBER, M.E. and PADDOCK, D. *J. Colloid Interface Sci.*, 94, (1983) p. 328.
27. LUTTRELL, G.H. and YOON, R.H. *J. Colloid Interface Sci.*, 154, (1992) p. 129.
28. NGUYEN VAN, A., RALSTON, J. and SCHULZE, H.J. *Int. J. Min. Proc.*, (in press).
29. DOBBY, G.S. and FINCH, J.A. *J. Colloid Interface Sci.*, 109, (1986) p. 493.
30. NGUYEN VAN, A. *Int. J. Min. Proc.* 37, (1993) p. 1.
31. SCHULZE, H.J. *Adv. Colloid Interface Sci.*, 40, (1992) p. 283.
32. HEWITT, D., FORNASIERO, D. and RALSTON, J. *J. Chem. Soc. Faraday Trans.*, 91 (13), 1997 (1995).
33. DOBBY, G.S. and FINCH, J.A. *Int. J. Miner. Process.*, 21, (1987) p. 241.
34. LEVIN, L.I. *Isd. Akad. Nauk SSR*, Moscow, (1961) (in Russian) p. 267.
35. LANGMUIR, J. and BLODGETT, K. *Gen. Elec. Comp. Rep.*, (1945).
36. DAI, Z., DUKHIN, S.S., FORNASIERO, D. and RALSTON, J. *J. Colloid Int. Sci.*, 197 (1998) p. 275.
37. DERJAGUIN, B.V. and DUKHIN, S.S. *Izv. Akad. Nauk OSSR, Otdel. Metall. Topl.* 1, (1959) p. 82.
38. FONDA, A. and HERNE, H. *Aerosol Science*, C.N. Davies (Ed.), Academic Press, London and New York, (1966) p. 393.
39. MICHAEL, D.H. and NOREY, P.W. *J. Fluid Mech.*, 37, part 3, (1969) p. 565.
40. SAMYGIN, V.D., CHERTILIN, B.S. and NEBERA, V.P. *Kolloidn. Zh.*, 39, (1977) p. 1101.
41. COLLINS, C.L. and JAMESON, G.L. *Chem. Eng. Sci.*, 32, (1977) p. 239.
42. YE, Y. and MILLER, J.D. *Coal Prep.*, 5, (1988) p. 147.
43. YE, Y. and MILLER, J.D. *Int. J. Miner. Process.*, 25, (1989) p. 199.
44. YOON, R.H. and LUTTRELL, G.H. *Mineral Process. and Extractive Metallurgy Review* 5, (1989) p. 101.
45. DUINEVELD, P.C. *J. Fluid Mechanics*, 292, (1995) p. 325.
46. SAM, A., GOMEZ, C.O. and FINCH, J.A. *Int. J. Miner. Proc.* 47, (1996) p. 177.
47. FLINT, L.R. and HOWARTH, W.J. *Chem. Eng. Sci.*, 26 (1971) p. 178. ◆

## Towards more user-friendly dredging charts

Andrews have developed charting methods to present minerals dredging information in a more detailed, user-friendly way—easily interpreted by the non-geologist. Such charts offer clearer guidance for the dredge operator, as they not only depict the precise positions of different soils, but show the depth and type of materials present, clearly colour-coded.

The service has been developed to assist the dredging contractor determine where to dredge and to what depths. The charts readily identify bedrock, sands, gravel and mineral-bearing soils with depths clearly shown. Little or no

knowledge of geology is needed to use the charts.

The clarity of presentation depends on several key survey components, which include accurate tidal information, using site gauges to reduce the bathymetric information, particularly with swathe bathymetry. Core samples need to be taken from the most geologically-representative locations, based on accurate interpretation.

Further details are available from Andrews, Salmon Road, Great Yarmouth, Norfolk, UK, NR30 3QS. Telephone 01493 332111. ◆